

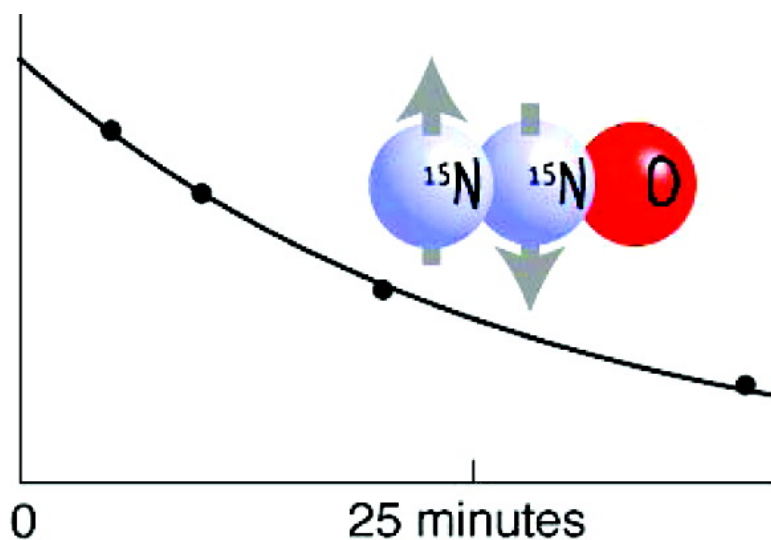
Communication

**The Long-Lived Nuclear Singlet State of N-Nitrous Oxide in Solution**

Giuseppe Pileio, Marina Carravetta, Eric Hughes, and Malcolm H. Levitt

*J. Am. Chem. Soc.*, **2008**, 130 (38), 12582-12583 • DOI: 10.1021/ja803601d • Publication Date (Web): 26 August 2008

Downloaded from <http://pubs.acs.org> on February 8, 2009



**More About This Article**

Additional resources and features associated with this article are available within the HTML version:

- Supporting Information
- Access to high resolution figures
- Links to articles and content related to this article
- Copyright permission to reproduce figures and/or text from this article

[View the Full Text HTML](#)

## The Long-Lived Nuclear Singlet State of $^{15}\text{N}$ -Nitrous Oxide in Solution

Giuseppe Pileio,<sup>†</sup> Marina Carravetta,<sup>†</sup> Eric Hughes,<sup>‡</sup> and Malcolm H. Levitt<sup>\*,†</sup>

School of Chemistry, University of Southampton, SO17 1BJ, Southampton, U.K., and Nestlé Research Centre, NESTEC LTD, 1000 Lausanne 26, Switzerland

Received May 14, 2008; E-mail: mhl@soton.ac.uk

Nuclear singlet states may have lifetimes  $T_S$  that exceed the conventional magnetization relaxation time  $T_1$  by an order of magnitude.<sup>1–11</sup> Applications of these states to the NMR measurements of slow molecular diffusion, chemical exchange, and the transport of hyperpolarized nuclear spin order have been demonstrated.<sup>8–11</sup>

So far, long-lived nuclear singlet states have only been observed for proton pairs. We now demonstrate an extraordinarily long lifetime ( $T_S$ ) of  $\sim 26$  min for the nuclear spin singlet of  $^{15}\text{N}_2$ -nitrous oxide (dinitrogen monoxide,  $\text{N}_2\text{O}$ ) in solution. This result has high potential importance since nitrous oxide is soluble in many important fluids such as water, oil, and blood. It is used routinely as a food additive, a gas propellant, and an anesthetic.

Doubly labeled  $^{15}\text{N}_2\text{O}$  gas, purchased from CK-gas (UK), was dissolved in a degassed solution of  $\text{DMSO}-d_6$  at a pressure of  $\sim 3.5$  bar. The concentration of  $^{15}\text{N}_2\text{O}$  in solution was  $\sim 0.3$  M as determined by comparison of the  $^{15}\text{N}$  signal strength with that from an external standard of  $^{15}\text{N}$ -benzamide. The  $^{15}\text{N}$  sites in  $^{15}\text{N}_2\text{O}$  are inequivalent and form a AX spin system with a difference in chemical shifts of  $\Delta\delta = 82.3$  ppm and a  $^{15}\text{N}$ – $^{15}\text{N}$  scalar coupling  $J = 8.1$  Hz. The  $^{15}\text{N}$  NMR spectrum, obtained in a magnetic field  $B_{\text{high}} = 7.0463$  T, is shown in Figure 1a.

The slow relaxation of singlet states is revealed by suppressing their interconversion with the triplet states, either by using a resonant radiofrequency field<sup>3–6</sup> or by reducing the static magnetic field to a very low value.<sup>1,2</sup> The radiofrequency method is not feasible for  $^{15}\text{N}_2\text{O}$  because of the large  $^{15}\text{N}$  chemical shift difference. The field-cycling procedure shown in Figure 2 was therefore used. This is a modified version of the method used in ref 1.

The spin system is allowed to reach thermal equilibrium, and two strong  $90^\circ$  pulses with a relative phase of  $90^\circ$  are applied at the mean chemical shift frequency of the two  $^{15}\text{N}$  sites. The delay between the pulses,  $\tau_1 = 0.198$  ms, was chosen so that the transverse magnetization vectors of the two  $^{15}\text{N}$  sites precess through  $180^\circ$  relative to each other. The two pulses act as a selective  $180^\circ$  pulse on one of the  $^{15}\text{N}$  sites and lead to a spin density operator<sup>10</sup> of the form

$$\hat{\rho}_2 \approx -\hat{I}_{jz} + \hat{I}_{kz} = |\beta\alpha\rangle\langle\beta\alpha| - |\alpha\beta\rangle\langle\alpha\beta| \quad (1)$$

where the two sites are denoted  $j$  and  $k$  and the selective inversion is assumed to act on site  $j$ . In this and the following equations, the subscript refers to a time point in Figure 2.

The sample is transported out of the magnetic field by activating a stepper motor to wind up a string attached to the sample holder. The transport process takes  $\tau_{\text{tr}} = 40$  s and transports the sample into a region of low magnetic field,  $B_{\text{low}} \approx 2$  mT, estimated by a Hall effect device. As shown in ref 2, slow adiabatic transport

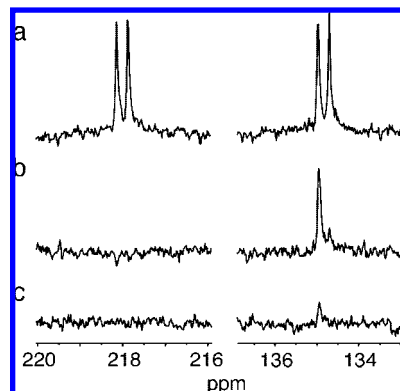


**Figure 1.**  $^{15}\text{N}$  spectra of  $^{15}\text{N}_2$ - $\text{N}_2\text{O}$  dissolved in  $\text{DMSO}-d_6$ : (a) conventional NMR spectrum taken using a single  $^{15}\text{N}$  pulse in a magnetic field of 7.04 T; (b) spectrum taken using the experimental sequence in Figure 2, with  $\tau_{\text{LF}} = 300$  s; (c) as in spectrum b but using  $\tau_{\text{LF}} = 40$  min. All spectra result from the sum of eight transients.

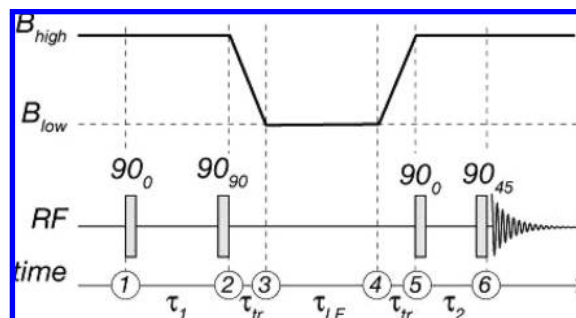


**Figure 2.** Field-cycling pulse sequence for observing the long-lived singlet state of  $^{15}\text{N}_2\text{O}$ . The circled numbers refer to time points mentioned in the text.

converts the population of each high-field state into that of the corresponding low-field state, leading to a density operator of the form

$$\hat{\rho}_3 \approx |S_0\rangle\langle S_0| - |T_0\rangle\langle T_0| \quad (2)$$

where the low-field eigenstates are  $|S_0\rangle = 2^{-1/2}(|\alpha\beta\rangle - |\beta\alpha\rangle)$ ,  $|T_{+1}\rangle = |\alpha\alpha\rangle$ ,  $|T_0\rangle = 2^{-1/2}(|\alpha\beta\rangle + |\beta\alpha\rangle)$ , and  $|T_{-1}\rangle = |\beta\beta\rangle$ . The sample is left in the low-field region for a variable time  $\tau_{\text{LF}}$ . During the first few minutes, the three triplet populations equilibrate with each other on a time scale set by the relaxation constant  $T_1$ . The density operator after several minutes in low magnetic field is therefore given approximately by

$$\hat{\rho}_4 \approx |S_0\rangle\langle S_0| - \frac{1}{3}|T_{+1}\rangle\langle T_{+1}| - \frac{1}{3}|T_0\rangle\langle T_0| - \frac{1}{3}|T_{-1}\rangle\langle T_{-1}| \quad (3)$$

The sample is transported back into the high-field region by running the stepper motor in the opposite direction. Adiabatic transport from the density operator in eq 3 leads to

<sup>†</sup> University of Southampton.

<sup>‡</sup> Nestlé Research Centre.

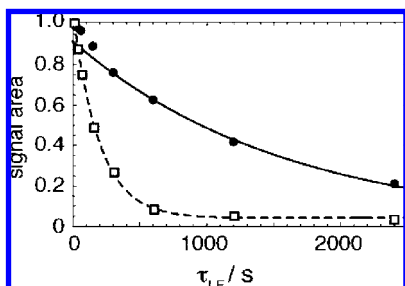


**Figure 3.** Decay of spin order in a saturated solution of  $^{15}\text{N}_2\text{-N}_2\text{O}$  in  $\text{DMSO-}d_6$ : (filled circles) decay of the singlet state; (empty squares) decay of total longitudinal magnetization.

$$\begin{aligned} \hat{\rho}_5 &\approx |\beta\alpha\rangle\langle\beta\alpha| - \frac{1}{3}|\alpha\alpha\rangle\langle\alpha\alpha| - \frac{1}{3}|\alpha\beta\rangle\langle\alpha\beta| - \frac{1}{3}|\beta\beta\rangle\langle\beta\beta| \\ &= -\frac{4}{3}I_{jz}I_k^\alpha + \frac{2}{3}I_k^\alpha - \frac{1}{3}\hat{1} \end{aligned} \quad (4)$$

When the sample is in position in high field, two strong  $90^\circ$  pulses with a relative phase of  $45^\circ$  are applied, separated by a delay  $\tau_2 = 0.099$  ms. This acts as a selective  $90^\circ$  pulse on site  $j$ , leading to the spin density operator

$$\hat{\rho}_6 \approx \frac{4}{3}I_{jz}I_k^\alpha + \frac{2}{3}I_k^\alpha - \frac{1}{3}\hat{1} \quad (5)$$

This corresponds to an NMR signal from only one of the two doublet components for site  $j$ , with no signals at all for site  $k$ . The experimental spectrum shown in Figure 1b has this approximate form. The advantage of this procedure is that the intensity of the single peak is 33% larger than generated in the conventional spectrum, neglecting relaxation losses.

The decay of the singlet state may be examined by increasing the low-field waiting time  $\tau_{\text{LF}}$ , while keeping all other events constant. The results are shown by the filled circles in Figure 3. The decay is exponential in the regime  $\tau_{\text{LF}} > 250$  s, with a decay time constant  $T_S = 1583 \pm 57$  s. The earlier time points are perturbed by the equilibration of the triplet populations, as explained above. Figure 1c shows a significant NMR signal even after 40 min in low field.

Figure 3 also shows the decay of conventional spin magnetization in the same low magnetic field. After equilibration in high field, the sample was transported out of the magnet and back in again, after waiting for a variable time  $\tau_{\text{LF}}$  in low field. A  $90^\circ$  pulse in high field was used to measure the remaining magnetization. The relaxation time constant for the total  $^{15}\text{N}$  magnetization is  $T_1 = 197 \pm 5$  s in the low magnetic field. The small residual signal at long waiting times is due to partial recovery of magnetization during the transport into the magnet. For comparison, the  $T_1$  values in a field of 7.0463 T are 198 and 114 s for the terminal and central positions, respectively.

The relaxation of  $^{15}\text{N}$  nuclei in  $^{15}\text{N}_2\text{O}$  is caused by a superposition of spin-rotation, chemical shift anisotropy, intramolecular dipole–dipole coupling, and external random field mechanisms. In low magnetic field, the chemical shift anisotropy mechanism is

absent, and the intramolecular dipole–dipole coupling does not cause singlet relaxation.<sup>1–7</sup> In a forthcoming publication we show that for pure spin-rotation relaxation,<sup>12</sup> the ratio of  $T_S$  and  $T_1$  is given by

$$T_S/T_1 = \frac{1}{2}(C_j^2 + C_k^2)/(C_j - C_k)^2 \quad (6)$$

where  $C_j$  and  $C_k$  are the spin-rotation tensors for the two  $^{15}\text{N}$  sites. This equation takes into account the strong cross-correlation of the spin-rotation interactions in this linear molecule. The values of the tensors are known<sup>13</sup> leading to an expected ratio  $T_S/T_1 = 11.4$ . The observed ratio  $T_S/T_1 = 8.0$  is qualitatively consistent with this. The remaining discrepancies are attributed to other relaxation mechanisms. Even slower singlet relaxation is expected for suitable larger molecules, for which even the conventional  $^{15}\text{N}$   $T_1$  may be as long as 500 s.<sup>14</sup>

We are now exploring the dependence of the  $^{15}\text{N}_2\text{O}$  singlet relaxation time on the solvent and the concentration of paramagnetic agents. For example, we have observed a  $T_S$  of  $\sim 19$  min for  $^{15}\text{N}_2\text{O}$  in undegassed olive oil.

Although the solubility of  $^{15}\text{N}_2\text{O}$  in blood at atmospheric pressure is about 15 times less than that observed under the current conditions, it should be possible to overcome this sensitivity loss by hyperpolarization techniques, enabling applications in medical imaging. The long singlet relaxation time of  $^{15}\text{N}$ -nitrous oxide should facilitate the transport of the agent to remote parts of the subject while minimizing the loss of nuclear spin order. Experiments are in progress for estimating the  $T_S$  in blood at different oxygenation levels, which might provide a contrast mechanism. Applications are also anticipated for following the diffusion and flow of materials such as oil and food substances.

**Acknowledgment.** This work is supported by EPSRC and URF/Royal Society. The authors wish to thank C. Godden, R. Dallay, J. James, A. Glass, O. G. Johannessen, and H. S. Vinay Deepak for experimental help.

## References

- (1) Carravetta, M.; Johannessen, O. G.; Levitt, M. H. *Phys. Rev. Lett.* **2004**, *92*, 153003.
- (2) Carravetta, M.; Levitt, M. H. *J. Chem. Phys.* **2005**, *122*, 214505.
- (3) Carravetta, M.; Levitt, M. H. *J. Am. Chem. Soc.* **2004**, *126*, 6228–6229.
- (4) Pileio, G.; Concistrè, M.; Carravetta, M.; Levitt, M. H. *J. Magn. Reson.* **2006**, *182*, 353–357.
- (5) Pileio, G.; Levitt, M. H. *J. Magn. Reson.* **2007**, *187*, 141–145.
- (6) Gopalakrishnan, K.; Bodenhausen, G. *J. Magn. Reson.* **2006**, *182*, 254–259.
- (7) Vinogradov, E.; Grant, A. K. *J. Magn. Reson.* **2007**, *188*, 176–182.
- (8) Cavadini, S.; Dittmer, J.; Antonijevic, S.; Bodenhausen, G. *J. Am. Chem. Soc.* **2005**, *127*, 5744–5748.
- (9) Sarkar, R.; Vasos, P. R.; Bodenhausen, G. *J. Am. Chem. Soc.* **2007**, *129*, 328–334.
- (10) Ahuja, P.; Sarkar, R.; Vasos, P. R.; Bodenhausen, G. *J. Chem. Phys.* **2007**, *127*, 134112.
- (11) Jonischkeit, T.; Bommerich, U.; Stadler, J.; Woelk, K.; Niessen, H. G.; Bargon, J. *J. Chem. Phys.* **2006**, *124*, 201109.
- (12) Hubbard, P. S. *Phys. Rev.* **1963**, *131*, 1155–1165.
- (13) Jameson, C. J.; Jameson, A. K.; Hwang, J. K.; Smith, N. C. *J. Chem. Phys.* **1988**, *89*, 5642–5648.
- (14) Mason, J. *Chem. Rev.* **1981**, *81*, 205–227.

JA803601D